Chapter 8

Nonlinear Optics

8.1 INTRODUCTION

The subject of polarization as related to reflection and transmission in isotropic homogeneous optical media such as optical glass was considered via Maxwell equations in Chapter 5. Here, we consider the subject of propagation and polarization in crystalline media, which gives origin to the subject of nonlinear optics. The brief treatment given here is at an introductory level and designed only to highlight the main features relevant to frequency conversion. For a detailed treatment on the subject of nonlinear optics, the reader is referred to a collection of books on nonlinear optics, including Bloembergen (1965), Baldwin (1969), Shen (1984), Yariv (1985), Mills (1991), Boyd (1992), and Agrawal (1995).

For propagation in an isotropic medium, the polarization P is related to the electric field by the following identity:

$$P = \chi^{(1)} E \tag{8.1}$$

where $\chi^{(1)}$ is known as the *electric susceptibility*.

In a crystal, the propagating field induces a polarization that depends on the direction and magnitude of this field, and the simple definition given in Eq. (8.1) must be amended to include the second- and third-order susceptibilities, so

$$P = \chi^{(1)}E + \chi^{(2)}E^2 + \chi^{(3)}E^3 + \ldots \tag{8.2}$$

Second-harmonic generation, sum-frequency generation, and optical parametric oscillation depend on $\chi^{(2)}$, while third-harmonic generation depends on $\chi^{(3)}$.

The second-order nonlinear polarization $\boldsymbol{P}^{(2)} = \chi^{(2)}\boldsymbol{E}^2$ can be expressed in more detail using

$$\boldsymbol{E}(t) = E_1 e^{-i\omega_1 t} + E_2 e^{-i\omega_2 t} + \ldots \tag{8.3}$$

according to Boyd (1992), so

$$\begin{aligned}\boldsymbol{P}^{(2)} = &\chi^{(2)}\Big(E_1^2 e^{-2i\omega_1 t} + E_2^2 e^{-2i\omega_2 t} + 2E_1E_2 e^{-i(\omega_1+\omega_2)t} + 2E_1E_2^* e^{-i(\omega_1-\omega_2)t} \\ &+2E_1^*E_2 e^{-i(\omega_1+\omega_2)t}\ldots\Big) + 2\chi^{(2)}\left(E_1E_1^* + E_2E_2^*\right)\end{aligned} \tag{8.4}$$

The first two terms of this equation relate to second-harmonic generation, the third term to sum-frequency generation, and the fourth term to difference-frequency generation.

Nonlinear susceptibility is described using tensors, which for the second order take the form of $\chi_{ijk}^{(2)}$. In shorthand notation these are described by

$$d_{ijk} = \frac{1}{2}\chi_{ijk}^{(2)} \tag{8.5}$$

In Table 8.1, second-order nonlinear susceptibilities are listed for some well-known crystals.

Identities useful in this chapter are

$$k_m = n_m\omega_m/c \tag{8.6}$$

$$k_m = 2\pi n_m/\lambda_m \tag{8.7}$$

$$n_m = \left(\varepsilon\omega_m\right)^{1/2} \tag{8.8}$$

Table 8.1

Second-Order Nonlinear Optical Susceptibilities[a,b]

Crystal	Point group	$d_{il} = \frac{1}{2}\chi^{(2)}$
ADP	42m	$d_{36} = 0.53$
KDP	42m	$d_{36} = 0.44$
$LiNbO_3$	3m	$d_{22} = 2.76, d_{31} = -5.44$
BBO	3m	$d_{22} = 2.22, d_{31} = 0.16$
KTP	mm2	$d_{31} = 6.5, d_{32} = 5.0 d_{33} = 13.7, d_{24} = 7.6, d_{15} = 6.1$
$AgGaS_2$	42m	$d_{36} = 13.4$
$AgGaSe_2$	42m	$d_{36} = 37.4$

Source: Barnes (1995).
[a] Units of d_{il} are in 10^{-12} m/V.
[b] The d_{il} matrix element is a contracted notation for d_{ijk} (see, for example, Boyd, 1992).

8.2 GENERATION OF FREQUENCY HARMONICS

Here, a basic description of second-harmonic, sum-frequency, and difference-frequency generation is given. The difference-frequency generation section is designed to describe some of the salient aspects of optical parametric oscillation.

8.2.1 Second-Harmonic and Sum-Frequency Generation

Previously, Maxwell equations were applied to describe propagation in isotropic linear optical media. Here the propagation of electromagnetic radiation in crystals is considered from a practical perspective consistent with the previous material on polarization.

Maxwell equations in the Gaussian system of units are given by (Born and Wolf, 1999)

$$\nabla \cdot \boldsymbol{B} = 0 \tag{8.9}$$

$$\nabla \cdot \boldsymbol{D} = 4\pi\rho \tag{8.10}$$

$$\nabla \times \boldsymbol{H} = (1/c)(\partial \boldsymbol{D}/\partial t + 4\pi \boldsymbol{j}) \tag{8.11}$$

$$\nabla \times \boldsymbol{E} = -(1/c)(\partial \boldsymbol{B}/\partial t) \tag{8.12}$$

For a description of propagation in a crystal we adopt the approach of Boyd (1992) and further consider a propagation medium characterized by $\rho = 0$, $\boldsymbol{j} = 0$, and $\boldsymbol{B} = \boldsymbol{H}$. The nonlinearity of the medium introduces

$$\boldsymbol{D} = \boldsymbol{E} + 4\pi \boldsymbol{P} \tag{8.13}$$

As in Chapter 5, taking the curl of both sides of Eq. (8.12) and using Eq. (8.13) leads to

$$\nabla \times \nabla \times \boldsymbol{E} = -c^{-2}\left(\nabla_t^2 \boldsymbol{E} + 4\pi \nabla_t^2 \boldsymbol{P}\right) \tag{8.14}$$

which is the generalized wave equation for nonlinear optics. Here, $\nabla_t^2 = (\partial^2/\partial t^2)$.

Following Boyd (1992), it is useful to provide a number of definitions starting by separating the polarization into its linear and nonlinear components,

$$\boldsymbol{P} = \boldsymbol{P}_L + \boldsymbol{P}_{NL} \tag{8.15}$$

followed by the separation of the displacement into

$$\boldsymbol{D} = \boldsymbol{D}_L + 4\pi \boldsymbol{P}_{NL} \tag{8.16}$$

where

$$D_L = E + 4\pi P_L \tag{8.17}$$

Using this definition, the nonlinear wave equation can be rewritten as

$$\nabla \times \nabla \times E = -c^{-2}\left(\nabla_t^2 D_L + 4\pi \nabla_t^2 P_{NL}\right) \tag{8.18}$$

In Chapter 5, for an isotropic material, we saw that

$$D_L = \varepsilon E \tag{8.19}$$

For the case of a crystal this definition can be modified to

$$D_L(r, t) = \varepsilon(\omega) \cdot E(r, t) \tag{8.20}$$

which includes a real frequency-dependent dielectric tensor. Using Eq. (8.20), the nonlinear wave equation can be restated as (Armstrong *et al.*, 1962)

$$\nabla \times \nabla \times E(r, t) = -c^{-2}\left(\varepsilon(\omega) \cdot \nabla_t^2 E(r, t) + 4\pi \nabla_t^2 P_{NL}(r, t)\right) \tag{8.21}$$

where

$$E(r, t) = E(r)e^{-i\omega t} + \ldots \tag{8.22}$$

$$P_{NL}(r, t) = P_{NL}(r)e^{-i\omega t} + \ldots \tag{8.23}$$

Now, with the nonlinear wave equation established, we proceed to describe the process of second-harmonic generation, or frequency doubling. This is illustrated schematically in Fig. 8.1 and consists of the basic process of radiation of ω_1 incident on a nonlinear crystal to yield collinear output radiation of frequency $\omega_2 = 2\omega_1$. We proceed, as in Chapter 5, using the identity

$$\nabla \times \nabla \times E = \nabla\nabla \cdot E - \nabla^2 E \tag{8.24}$$

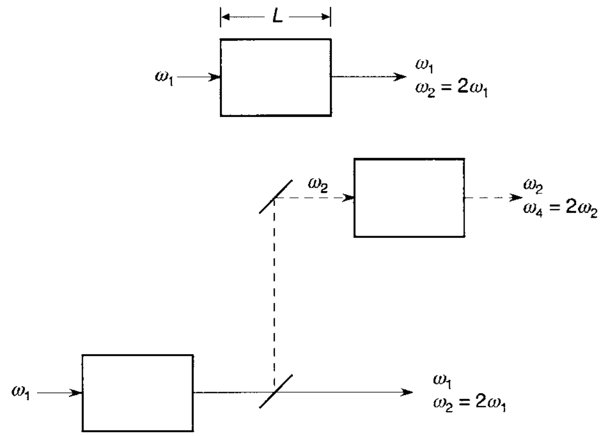

Figure 8.1 Optical configuration for frequency-doubling generation.

the wave equation can be restated in scalar form as

$$\nabla^2 E_m(z,t) = -c^{-2}\big(\varepsilon(\omega_m)\nabla_t^2 E_m(z,t) + 4\pi\nabla_t^2 P_m(z,t)\big) \tag{8.25}$$

After Boyd (1992), we use the following expressions for $m = 2$:

$$E_m(z,t) = A_m(z)e^{ik_m z}e^{-i\omega_m t} + \ldots \tag{8.26}$$

$$E(z,t) = E_1(z,t) + E_2(z,t) \tag{8.27}$$

$$P_m(z,t) = P_m(z)e^{-i\omega_m t} + \ldots \tag{8.28}$$

$$P_1(z) = 4dA_2A_1^*e^{i(k_2-k_1)z} \tag{8.29}$$

$$P_2(z) = 2dA_1^2e^{ik_1z} \tag{8.30}$$

$$P(z,t) = P_1(z,t) + P_2(z,t) \tag{8.31}$$

Following differentiation and substitution into the wave equation, the $\partial^2 A_1/\partial z^2$ and $\partial^2 A_2/\partial z^2$ terms are neglected, so the coupled-amplitude equations can be expressed as (Boyd, 1992)

$$dA_1/dz = i(8\pi d\omega_1^2/k_1c^2)A_1^*A_2e^{-i\Delta kz} \tag{8.32}$$

$$dA_2/dz = i(4\pi d\omega_2^2/k_2c^2)A_1^2e^{i\Delta kz} \tag{8.33}$$

where

$$\Delta k = 2k_1 - k_2 \tag{8.34}$$

Integration of Eq. (8.33) leads to

$$A_2A_2^* = (4\pi d\omega_2^2/k_2c^2)^2A_1^4L^2\left[\left(\sin^2(L\Delta k/2)\right)/(L\Delta k/2)^2\right] \tag{8.35}$$

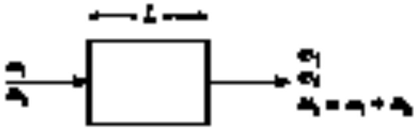

Figure 8.2 Optical configuration for sum-frequency generation.

Equation (8.35) illustrates the nonlinear dependence of the frequency-doubled output on the input signal and indicates its relation to the $(L\Delta k/2)$ parameter. This dependence implies that conversion efficiency decreases significantly as $(L\Delta k/2)$ increases. The distance

$$L_c = 2/\Delta k \tag{8.36}$$

referred to as the *coherence length* of the crystal, provides a measure of the length of the crystal necessary for the efficient generation of second-harmonic radiation.

Sum-frequency generation is outlined in the third term of Eq. (8.4) and involves the interaction of radiation at two different frequencies in a crystal to produce radiation at a third distinct frequency. This process, illustrated schematically in Fig. 8.2, consists of the coaxial incidence radiation of ω_1 and ω_2 onto a nonlinear crystal to yield collinear output radiation of frequency $\omega_3 = \omega_1 + \omega_2$. Using the appropriate expressions for $E_m(z,t)$ and $P_m(z,t)$ in the wave equation, it can be shown that (Boyd, 1992)

$$\Delta k = k_1 + k_2 - k_3 \tag{8.37}$$

and the output intensity again depends on $\mathrm{sinc}^2(L\Delta k/2)$.

The ideal condition of *phase matching* is achieved when

$$\Delta k = 0 \tag{8.38}$$

and it offers the most favorable circumstances for a high conversion efficiency. When this condition is not satisfied, there is a strong decrease in the efficiency of sum-frequency generation.

8.2.2 Difference-Frequency Generation and Optical Parametric Oscillation

The process of difference-frequency generation is outlined in the fourth term of Eq. (8.4) and involves the interaction of radiation at two different frequencies in a crystal to produce radiation at a third distinct frequency. This process, illustrated schematically in Fig. 8.3, consists of the coaxial incidence

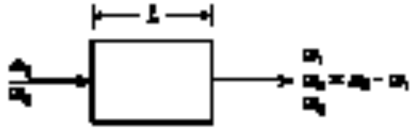

Figure 8.3 Optical configuration for difference-frequency generation.

radiation of ω_3 and ω_1 onto a nonlinear crystal to yield nonlinear output radiation of frequency $\omega_2 = \omega_3 - \omega_1$.

Assuming that ω_3 is the frequency of a high-intensity pump-laser beam, which remains undepleted during the excitation process, then A_3 can be considered a constant; using an analogous approach to that adopted in the previous section, it is found that (Boyd, 1992)

$$dA_1/dz = i(8\pi d\omega_1^2/k_1c^2)A_3A_2^*e^{i\Delta kz} \tag{8.39}$$

$$dA_2/dz = i(8\pi d\omega_2^2/k_2c^2)A_3A_1^*e^{i\Delta kz} \tag{8.40}$$

$$dA_3/dz = 0 \tag{8.41}$$

where

$$\Delta k = k_3 - k_2 - k_1 \tag{8.42}$$

If the nonlinear crystal involved in the process of frequency difference is deployed and properly aligned at the propagation axis of an optical resonator, as illustrated in Fig. 8.4, then the intracavity intensity can build to very high values. This is the essence of an *optical parametric oscillator* (OPO). Early papers on OPOs are those of Giordmaine and Miller (1965), Akhmanov *et al.* (1965), Byer *et al.* (1968), and Harris (1969). Recent reviews are given by Barnes (1995) and Orr *et al.* (1995).

In the OPO literature, ω_3 is known as the *pump* frequency, ω_1 as the *idler* frequency, and ω_2 as the *signal* frequency. Thus, Eq. (8.42) can be restated as

$$\Delta k = k_p - k_s - k_i \tag{8.43}$$

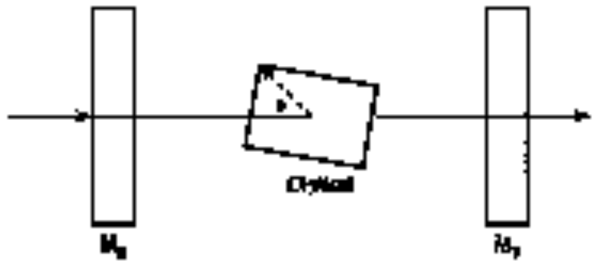

Figure 8.4 Basic optical parametric oscillator configuration.

Equations (8.39) and (8.40) can be used to provide equations for the signal under various conditions of interest. For example, for the case when the initial idler intensity is zero and $\Delta k \approx 0$, it can be shown that

$$A_S(L)A_S^*(L) \approx \frac{1}{4} A_S(0)A_S^*(0)\left(e^{\gamma L} + e^{-\gamma L}\right)^2 \tag{8.44}$$

where $A_S(0)$ is the initial amplitude of the signal. Here, the parameter γ is defined as (Boyd, 1992)

$$\gamma = \left(64\pi^2 d^2 \omega_I^2 \omega_S^2 k_I^{-1} k_S^{-1} c^{-4} |A_P|^2\right)^{1/2} \tag{8.45}$$

Equation (8.44) indicates that for the ideal condition of $\Delta k \approx 0$, the signal experiences an exponential gain as long as the *pump* intensity is not depleted.

Frequency selectivity in pulsed OPOs has been studied in detail by Brosnan and Byer (1979) and Barnes (1995). Wavelength tuning by angular and thermal means is discussed by Barnes (1995). Considering the frequency difference

$$\omega_S = \omega_P - \omega_I \tag{8.46}$$

and Eq. (8.43), it can be shown that for the case of $\Delta k \approx 0$ (Orr *et al.*, 1995),

$$\lambda_S = \lambda_P(n_S - n_I)/(n_P - n_I) \tag{8.47}$$

which illustrates the dependence of the signal wavelength on the refractive indices. An effective avenue to change the refractive index is to vary the angle of the optical axis of the crystal relative to the optical axis of the cavity, as indicated in Fig. 8.4. For instance, Brosnan and Byer (1979) report that changing this angle from 45° to 49° in a Nd:YAG laser–pumped $LiNbO_3$ OPO tunes the wavelength from $\sim 2\ \mu m$ to beyond $4\ \mu m$. The angular dependence of refractive indices in uniaxial birefringent crystals is discussed by Born and Wolf (1999).

It should be mentioned that the principles discussed in Chapters 6 and 7 can be applied toward the tuning and linewidth narrowing in OPOs. However, there are some unique features of nonlinear crystals that should be considered in some detail. Central to this discussion is the issue of phase matching, or allowable mismatch. It is clear that a resonance condition exists around $\Delta k \approx 0$, and from Eq. (8.44) it is seen that the output signal from an OPO can experience a large increase when this condition is satisfied. Thus, $\Delta k \approx 0$ is a desirable feature. Here it should be mentioned that some authors define slightly differently what is known as *allowable mismatch*. For instance, Barnes (1995) defines it as

$$\Delta k = \pi/L \tag{8.48}$$

which is slightly broader than the definition given in Eq. (8.36).

The discussion on frequency selectivity in OPOs benefits significantly by expanding Δk in a Taylor series (Barnes and Corcoran, 1976) so that

$$\Delta k = \Delta k_0 + (\partial \Delta k/\partial x)\Delta x + (1/2!)(\partial^2 \Delta k/\partial x^2)\Delta x^2 + \ldots \tag{8.49}$$

Here this process is repeated for other variables of interest

$$\Delta k = \Delta k_0 + (\partial \Delta k/\partial \theta)\Delta \theta + (1/2!)(\partial^2 \Delta k/\partial \theta^2)\Delta \theta^2 + \ldots \tag{8.50}$$

$$\Delta k = \Delta k_0 + (\partial \Delta k/\partial \lambda)\Delta \lambda + (1/2!)(\partial^2 \Delta k/\partial \lambda^2)\Delta \lambda^2 + \ldots \tag{8.51}$$

$$\Delta k = \Delta k_0 + (\partial \Delta k/\partial T)\Delta T + (1/2!)(\partial^2 \Delta k/\partial T^2)\Delta T^2 + \ldots \tag{8.52}$$

Equating the first two series and ignoring the second derivatives, it is found that (Barnes, 1995)

$$\Delta \lambda = \Delta \theta(\partial \Delta k/\partial \theta)(\partial \Delta k/\partial \lambda)^{-1} \tag{8.53}$$

This linewidth equation shows a dependence on the beam divergence, which is determined by the geometrical characteristics of the pump beam and the geometry of the cavity. It should be noted that this equation provides an estimate of the *intrinsic linewidth* available from an OPO in the absence of intracavity dispersive optics or injection seeding from external sources. Barnes (1995) reports that for a $AgGaSe_2$ OPO pumped by a Ho:YLF laser, the linewidth is $\Delta\lambda \approx 0.0214\,\mu m$ at $\lambda \approx 3.82\,\mu m$.

Introduction of the intracavity dispersive techniques described in Chapter 7 produce much narrower emission linewidths. A dispersive OPO is illustrated in Fig. 8.5. For this oscillator the multiple-return-pass linewidth is determined by

$$\Delta \lambda = \Delta \theta_R (RM\nabla_\lambda \Theta_G + R\nabla_\lambda \Phi_P)^{-1} \tag{8.54}$$

where the various coefficients are as defined in Chapter 7. It should be apparent that Eq. (8.54) has its origin in

$$\Delta \lambda = \Delta \theta(\partial \theta/\partial \lambda)^{-1} \tag{8.55}$$

which is a simplified version of Eq. (8.53). Hence, we have demonstrated a simple mathematical approach to arrive at the linewidth equation that was derived using geometrical arguments in Chapter 4.

Using a dispersive cavity incorporating an intracavity etalon in a $LiNbO_3$ OPO excited by a Nd:YAG laser, Brosnan and Byer (1979) achieved a linewidth of $\Delta\nu \approx 2.25$ GHz. Also using a Nd:YAG-pumped $LiNbO_3$ OPO and a similar interferometric technique, Milton *et al.* (1989) achieved single-longitudinal-mode emission at a linewidth of $\Delta\nu \approx 30$ MHz.

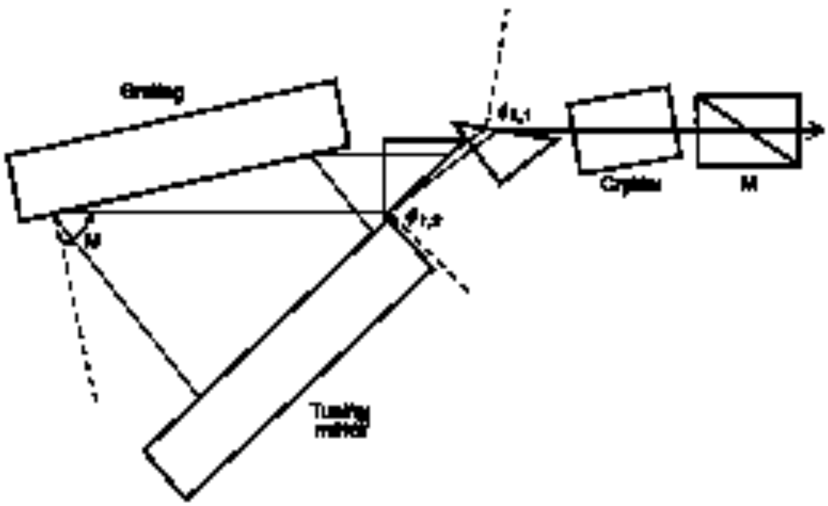

Figure 8.5 Dispersive optical parametric oscillator using an HMPGI grating configuration.

A further aspect illustrated by the Taylor series expansion is that by equating the second and third series it is found that

$$\Delta\theta = \Delta T(\partial\Delta k/\partial T)(\partial\Delta k/\partial\theta)^{-1} \tag{8.56}$$

which indicates that the beam divergence is a function of temperature, which should be considered when contemplating thermal tuning techniques. Chapter 9 includes a section on the emission performance of various OPOs.

8.2.3 The Refractive Index as a Function of Intensity

Using a Taylor series to expand an expression for the refractive index yields

$$n = n_0 + (\partial n/\partial I)I + (1/2!)(\partial^2 n/\partial I^2)I^2 + \ldots \tag{8.57}$$

Neglecting the second-order and higher terms, this expression reduces to

$$n = n_0 + (\partial n/\partial I)I \tag{8.58}$$

where n_0 is the normal weak-field refractive index, defined in Chapter 12 for various materials. The quantity $(\partial n/\partial I)$ is not dimensionless and has units that are the inverse of the laser intensity, or $W^{-1}\ cm^2$. Using polarization arguments this derivative can be expressed as (Boyd, 1992)

$$\partial n/\partial I = 12\pi^2\chi^3/(n_0^2(\omega)c) \tag{8.59}$$

This quantity is known as the *second-order index of refraction* and is traditionally referred to as n_2. Setting $\partial n/\partial I = n_2$, Eq. (8.58) can be restated in its usual form as

$$n(\omega) = n_0(\omega) + n_2(\omega)I(\omega) \tag{8.60}$$

The change in refractive index as a function of laser intensity is known as the *optical Kerr effect*. For a description of the electro-optical Kerr effect, the reader should refer to Agrawal (1995).

A well-known consequence of the optical Kerr effect is the phenomenon of *self-focusing*. This results from the propagation of a laser beam with a near-Gaussian spatial intensity profile, since, according to Eq. (8.60), the refractive index at the center of the beam is higher than the refractive index at the wings of the beam. This results in an intensity-dependent lensing effect, as illustrated in Fig. 8.6.

The phenomenon of self-focusing, or intensity-dependent lensing, is important in ultrafast lasers or femtosecond lasers (Diels, 1990; Diels and Rudolph, 1996), where it gives rise to what is known as *Kerr lens mode locking* (KLM). This is applied to spatially select the high-intensity mode-locked pulses from the background CW lasing. This can be accomplished simply by inserting an aperture near the gain medium to restrict lasing to the central, high-intensity, portion of the intracavity beam. This technique has become widely used in femtosecond laser cavities.

8.3 OPTICAL PHASE CONJUGATION

Optical phase conjugation is a technique that is applied to correct laser beam distortions either intracavity or extracavity. A proof of the distortion correction properties of phase conjugation was provided by Yariv (1977) and is

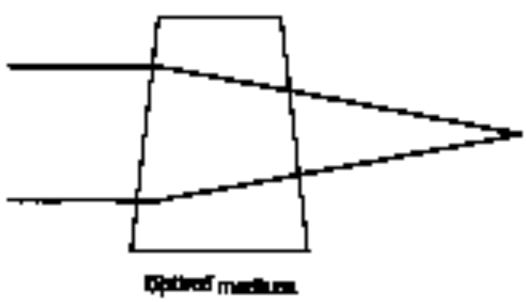

Figure 8.6 Simplified representation of self-focusing due to $n = n_0 + n_2I$ in an optical medium due to propagation of a laser beam with a near-Gaussian intensity profile.

outlined here. Consider a propagating beam in the $+z$ direction, represented by

$$E(r,t) = A_1(r)e^{-i(\omega t - kz)} + \ldots \tag{8.61}$$

and the scalar version of the nonlinear wave equation given in Eq. (8.25), assuming that the spatial variations of ϵ are much larger than the optical wavelength. Neglecting the polarization term one can write

$$(\partial^2 A_1/\partial z^2) + i2k(\partial A_1/\partial z) + \left((\epsilon\omega^2/c^2) - k^2\right)A_1 = 0 \tag{8.62}$$

The complex conjugate of this equation is

$$(\partial^2 A_1^*/\partial z^2) - i2k(\partial A_1^*/\partial z) + \left((\epsilon\omega^2/c^2) - k^2\right)A_1^* = 0 \tag{8.63}$$

which is the same wave equation as for a wave propagating in the $-z$ direction of the form

$$E(r,t) = A_2(r)e^{-i(\omega t + kz)} + \ldots \tag{8.64}$$

provided

$$A_2(r) = aA_1^*(r) \tag{8.65}$$

where a is a constant. Here, the presence of a distorting medium is represented by the *real* quantity ϵ (Yariv, 1977). This exercise illustrates that a wave propagating in the *reverse direction* of $A_1(r)$ and whose complex amplitude is *everywhere* the complex conjugate of $A_1(r)$ satisfies the same wave equation satisfied by $A_1(r)$. From a practical perspective this implies that a phase-conjugate mirror can generate a wave propagating in reverse to the incident wave whose amplitude is the complex conjugate of the incident wave. Thus, the wavefronts of the reverse wave coincide with those of the incident wave. This concept is illustrated in Fig. 8.7.

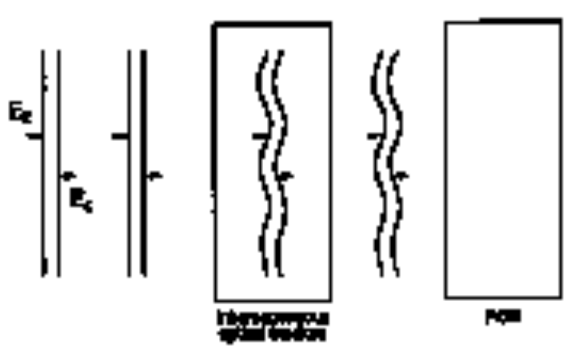

Figure 8.7 The concept of optical phase conjugation.

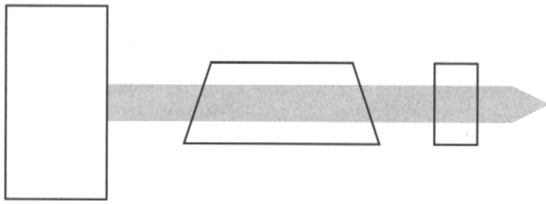

Figure 8.8 Basic phase-conjugated laser cavity.

A phase-conjugated mirror (PCM), as depicted in Fig. 8.8, is generated by a process called *degenerate four-wave mixing* (DFWM), which itself depends on $\chi^{(3)}$ (Yariv, 1985). This process can be described by considering plane-wave equations of the form

$$E_m(r,t) = A_m(r)e^{-i(\omega t - k_m \cdot r)} + \ldots \tag{8.66}$$

where $m = 1, 2, 3, 4$ and k and r are vectors. Using these equations and the simplified equations for the four polarization terms (Boyd, 1992),

$$P_1 = 3\chi^{(3)}[E_1^2 E_1^* + 2E_1 E_2 E_2^*] \tag{8.67a}$$

$$P_2 = 3\chi^{(3)}[E_2^2 E_2^* + 2E_2 E_1 E_1^*] \tag{8.67b}$$

$$P_3 = 3\chi^{(3)}[2E_3 E_1 E_1^* + 2E_3 E_2 E_2^* + 2E_1 E_2 E_4^*] \tag{8.67c}$$

$$P_4 = 3\chi^{(3)}[2E_4 E_1 E_1^* + 2E_4 E_2 E_2^* + 2E_1 E_2 E_3^*] \tag{8.67d}$$

in the generalized wave equation

$$\nabla^2 E_m(z,t) = -c^{-2}\left(\varepsilon(\omega_m)\nabla_t^2 E_m(z,t) + 4\pi\nabla_t^2 P_m(z,t)\right)$$

eventually leads to expressions for the amplitudes that show that the generated field is driven only by the complex conjugate of the input amplitude.

An issue of practical interest is the representation of a phase-conjugated mirror in transfer-matrix notation, as introduced in Chapter 6. This problem was solved by Auyeung *et al.* (1979), who, using the argument that the reflected field is the conjugate replica of the incident field, showed that the *ABCD* matrix is given by

$$\begin{pmatrix} A & B \\ C & D \end{pmatrix} = \begin{pmatrix} 1 & 0 \\ 0 & -1 \end{pmatrix} \tag{8.68}$$

which should be compared to

$$\begin{pmatrix} A & B \\ C & D \end{pmatrix} = \begin{pmatrix} 1 & 0 \\ 0 & 1 \end{pmatrix} \tag{8.69}$$

for a conventional optical mirror. A well-known nonlinear material suitable as a PCM is CS_2 (Yariv, 1985). Fluctuations in the phase-conjugated signal generated by DFWM in sodium was investigated by Kumar et al. (1984).

8.4 RAMAN SHIFTING

Stimulated Raman scattering (SRS) is an additional and very useful tool to extend the frequency range of fixed-frequency and tunable lasers. Also known as Raman shifting, SRS can be accomplished by focusing a TEM_{00} laser beam onto a nonlinear medium, such as H_2 (as illustrated in Fig. 8.9), to generate emission at a series of wavelengths above and below the wavelength of the laser pump. The series of longer-wavelength emissions are known as Stokes and are determined by (Hartig and Schmidt, 1979)

$$\nu_{S_m} = \nu_P - m\nu_R \tag{8.70}$$

where ν_{S_m} is the frequency of a given Stokes, ν_P is the frequency of the pump laser, ν_R is the intrinsic Raman frequency, and $m = 1, 2, 3, 4 \ldots$ for successively higher Stokes. For the series of shorter anti-Stokes wavelengths,

$$\nu_{AS_m} = \nu_P + m\nu_R \tag{8.71}$$

where ν_{AS_m} is the frequency of a given anti-Stokes. It should be noted that ν_{S_1} and ν_{AS_1} are generated by the pump radiation, while these fields, in turn, generate ν_{S_2} and ν_{AS_2}. In other words, for $m = 2, 3, 4, \ldots$, ν_{S_m} and ν_{AS_m} are generated by $\nu_{S_{(m-1)}}$ and $\nu_{AS_{(m-1)}}$, respectively. Hence, the most intense radiation occurs for $m = 1$, with successively weaker emission for $m = 2, 3, 4, \ldots$, as depicted in Fig. 8.10. For instance, efficiencies can decrease progressively from 37% (first Stokes), to 18% (second Stokes), to 3.5% (third Stokes) (Bénit et al., 1985). For the H_2 molecule, $\nu_R \approx 124.5637863$ THz (or 4155 cm^{-1}) (Bloembergen, 1967).

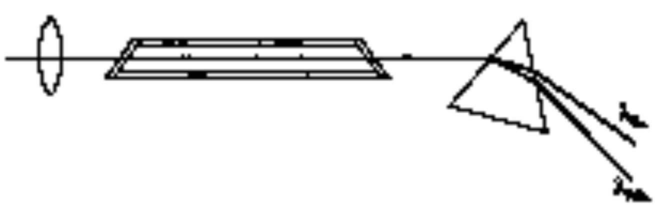

Figure 8.9 Optical configuration for H_2 Raman shifter. The output window and the dispersive prism are made of CaF_2.

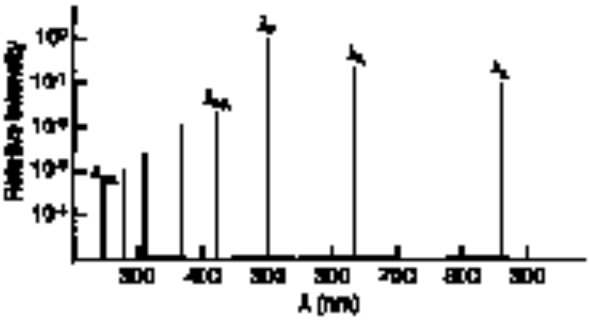

Figure 8.10 Stokes and anti-Stokes emission in H_2 for $\lambda_p = 500$ nm.

Using the wave equation and assuming solutions of the form

$$E_S(z,t) = A_S(z)e^{-i(\omega_S t - k_S z)} + \ldots \quad (8.72)$$

$$E_P(z,t) = A_P(z)e^{-i(\omega_P t - k_P z)} + \ldots \quad (8.73)$$

it can be shown, using the fact that the Stokes polarization depends on $\chi^{(3)}E_P E_P^* E_S$, that the gain at the Stokes frequency depends on the intensity of the pump radiation, the population density, and the inverse of the Raman linewidth, among other factors (Trutna and Byer, 1980). It is interesting to note that the Raman gain can be independent of the linewidth of the pump laser (Trutna *et al.*, 1979). A detailed description on the mechanics of SRS is provided by Boyd (1992).

Stimulated Raman Scattering in H_2 has been widely used to extend the frequency range of tunable lasers, such as dye lasers. This technique was first demonstrated by Schmidt and Appt (1972) using room-temperature hydrogen at a pressure of 200 atmospheres. This is mentioned because, though simple, the use of pressurized hydrogen requires stainless steel cells and detailed attention to safety procedures. Using a dye laser with an emission wavelength centered around 563 nm, Wilke and Schmidt (1978) generated SRS radiation in H_2 from the eight anti-Stokes (at 198 nm) to the third Stokes (at 2064 nm) at an overall conversion efficiency of up to 50%. Using the second harmonic of the dye laser, the same authors generated from the fourth anti-Stokes to the fifth Stokes, as illustrated on Table 8.2, at an overall conversion efficiency of up to 75%. Using a similar dye laser configuration, Hartig and Schmidt (1979) employed a capillary waveguide H_2 cell to generate tunable first, second, and third Stokes spanning the wavelength range from 0.7 µm to 7 µm.

Using a dye laser system incorporating a MPL grating oscillator and two stages of amplification, Schomburg *et al.* (1982) achieved generation up to the thirteenth anti-Stokes at 133 nm. Brink and Proch (1982) report on a 70%

Table 8.2

Tunable Raman Shifting in Hydrogen

Anti-Stokes λ range (nm)	Tunable laser[a] λ range (nm)	Stokes λ range (nm)[b]
$\lambda_4 \approx 192$ ($\delta\lambda_4 \approx 5.8$)[c]	$275 \leq \lambda \leq 287$	$309 \leq \lambda_1 \leq 326$
$\lambda_3 \approx 210$ ($\delta\lambda_3 \approx 7.2$)		$350 \leq \lambda_2 \leq 379$
$\lambda_2 \approx 229$ ($\delta\lambda_2 \approx 8.9$)		$418 \leq \lambda_3 \leq 450$
$\lambda_1 \approx 251$ ($\delta\lambda_1 \approx 10.7$)		$505 \leq \lambda_4 \leq 550$
		$640 \leq \lambda_5 \leq 701$

Source: Wilke and Schmidt (1978).
[a] Second harmonic from a dye laser.
[b] Approximate values.
[c] Corresponds to a quoted range of 188.7 nm $\leq \lambda_4 \leq$ 196.5 nm. All other values are approximate.

conversion efficiency at the seventh anti-Stokes by lowering the H_2 temperature to 78°K. Hanna *et al.* (1985) report on a 90% conversion efficiency to the first Stokes using an oscillator-amplifier configuration for SRS in H_2.

In addition to H_2, numerous materials have been characterized as SRS media (Bloembergen, 1967; Yariv, 1975). Other gaseous media include I_2 (Fouche and Chang, 1972), Cs (Wyatt and Cotter, 1980), Ba (Manners, 1983), Sn and Tl (White and Henderson, 1983; Ludewigt *et al.*, 1984), and Pb (Marshall and Piper, 1990). Stimulated Raman Scattering in optical fibers is discussed in detail by Agrawal (1995).

8.5 APPLICATIONS OF NONLINEAR OPTICS

Perhaps the most well-known application of nonlinear optics in the field of laser optics is in the generation of second, third, and fourth harmonics of some well-established laser sources, such as the Nd:YAG laser. Table 8.3 lists the laser fundamental and its three harmonics. This frequency multiplication can be accomplished using nonlinear crystals, such as KDP and ADP. Certainly, it should be apparent that the generation of frequency harmonics is not limited to just the Nd:YAG laser, it is also practiced with a variety of laser sources, including tunable lasers.

One application that integrates various aspects of laser optics, including harmonic generation, is known as *optical clockwork* (Holzwarth *et al.*, 2001). This involves the generation of a phase-locked white-light continuum for absolute frequency measurements. This is an idea originally outlined by Hänsch and colleagues in the mid- to late 1970s (Eckstein *et al.*, 1978) but

Table 8.3

Harmonics of the $^4F_{3/2}$–$^4I_{11/2}$ Transition of the Nd:YAG Laser

Fundamental	Harmonics
$\nu \approx 2.82 \times 10^{14}$ Hz ($\lambda \approx 1064$ nm)	$2\nu \approx 5.64 \times 10^{14}$ Hz ($\lambda \approx 532$ nm)
	$3\nu \approx 8.46 \times 10^{14}$ Hz ($\lambda \approx 355$ nm)
	$4\nu \approx 1.13 \times 10^{15}$ Hz ($\lambda \approx 266$ nm)

only recently has found the technological tools necessary to become significantly developed.

The basic tools are a stabilized femtosecond laser, a nonlinear crystal fiber capable of self-modulation, a stabilized narrow-linewidth laser, and a frequency-doubling crystal. Briefly, the concept consists of generating a periodic train of pulses, also known as a *comb* or *ruler*, with each pulse separated by an interval Δ, for an entire optical octave. This is accomplished by focusing a high-intensity femtosecond laser beam on to a $\chi^{(3)}$ medium. This medium is a crystal fiber, also known as a *photonic crystal fiber* (PCF), whose refractive index behaves according to

$$n(I) = n_0 + n_2 I(t) \tag{8.74}$$

Propagation in such a medium causes red spread at the leading edge of the pulse and a blue spread at the trailing edge of the pulse, since the field experiences a time-dependent shift according to (Bellini and Hänsch, 2000)

$$\Delta\omega(t) = -(\omega_0 n_2 L/c)(dI(t)/dt) \tag{8.75}$$

Thus, a high-intensity ~20-fs pulse focused on a $\chi^{(3)}$ medium a few centimeters long can give rise to a continuum (Holzwarth *et al.*, 2001).

The stabilized-frequency and broadened pulse train is made collinear with a narrow-linewidth stabilized laser, to be measured, and its second harmonic (Diddams *et al.*, 2000). The combined laser beam containing the pulse train ν and 2ν is then dispersed by a grating, and two detectors are combined to determine the frequency beating between the pulse train with ν and 2ν, thus determining the beat frequencies δ_1 and δ_2 (see Fig. 8.11). Following Diddams *et al.* (2000), the frequency difference is given by

$$2\nu - \nu = n\Delta \pm (\delta_1 \pm \delta_2) \tag{8.76}$$

where

$$\Delta = v_g/2L \tag{8.77}$$

is determined by controlling L, which is the cavity length of the stabilized femtosecond laser. Using this method, Diddams *et al.* (2000) determined

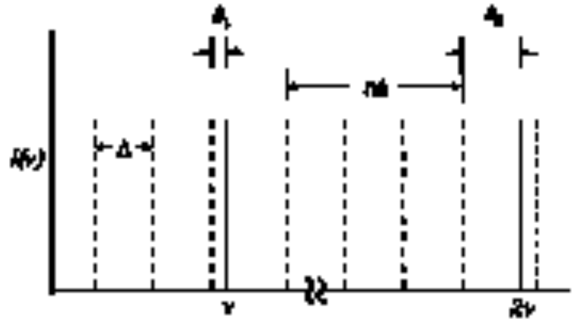

Figure 8.11 Schematics for determining the frequency difference $(2\nu - \nu)$ in the optical clockwork. (Adapted from Diddams *et al.*, 2000.)

ν for an $^{127}I_2$-stabilized Nd:YAG laser to be 281, 630, 111, 740 kHz, with an offset of +17.2 kHz.

This technique has led to the development of optical frequency synthesizers capable of providing an upper limit for the measurement uncertainty of several parts in 10^{-16} (Holzwarth *et al.*, 2000). The method has also been extended to include other stabilized lasers and higher harmonics (Holzwarth *et al.*, 2001).

PROBLEMS

1. Use Maxwell's equations to derive the generalized wave equation of nonlinear optics, that is, Eq. (8.14).
2. Use Eq. (8.40) to arrive at Eq. (8.44) using the approximation $\Delta k \approx 0$.
3. Use the scalar form of the wave equation [Eq. (8.25)] to arrive at Eq. (8.62).
4. Derive the linewidth equation for an OPO, that is, Eq. (8.53).
5. Determine the wavelengths for the Stokes radiation at $n = 1, 2, 3$ and for the anti-Stokes radiation at $n = 1, 2, 3, 4, 5$ for H_2, given that the laser excitation is at $\lambda = 500$ nm.

REFERENCES

Agrawal, G. P. (1995). *Nonlinear Fiber Optics*, 2nd ed. Academic Press, New York.

Akhmanov, S. A., Kovrigin, A. I., Kolosov, V. A., Piskarskas, A. S., Fadeev, V. V., Khokhlov, R. V. (1966). Tunable parametric light generator with KDP crystal. *JETP Lett.* **3**, 241–245.

Armstrong, J. A., Bloembergen, N., Ducuing, J., and Pershan, P. S. (1962). Interactions between light waves in a nonlinear dielectric. *Phys. Rev.* **127**, 1918–1939.

Auyeung, J., Fekete, D., Pepper, D. M., and Yariv, A. (1979). A theoretical and experimental investigation of the modes of optical resonators with phase-conjugate mirrors. *IEEE J. Quantum Electron.* QE-15, 1180–1188.

Baldwin, G. C. (1969). *An Introduction to Nonlinear Optics*. Plenum Press, New York.

Barnes, N. P. (1995a). Transition metal solid-state lasers. In *Tunable Lasers Handbook* (Duarte, F. J., ed.). Academic Press, New York, pp. 219–291.

Barnes, N. P. (1995b). Optical parametric oscillators. In *Tunable Lasers Handbook* (Duarte, F. J., ed.). Academic Press, New York, pp. 293–348.

Barnes, N. P., and Corcoran, V. J. (1976). Parametric generation processes: spectral bandwidth and acceptance angles. *Appl. Opt.* 15, 696–699.

Bellini, M., and Hänsch, T. W. (2000). Phase-locked white-light continuum pulses: toward a universal optical frequency-comb synthesizer. *Opt. Lett.* 25, 1049–1051.

Batin, B., Davidenko, B., Mikhailov, V., Apanasevich, P., Grabchikov, A., and Orlovich, V. (1985). Stimulated Raman scattering of dye laser radiation in hydrogen: improvement of spectral purity. *Opt. Commun.* 56, 285–287.

Bloembergen, N. (1965). *Nonlinear Optics*. Benjamin, New York.

Bloembergen, N. (1967). The stimulated Raman effect. *Am. J. Phys.* 35, 989–1023.

Boyd, R. W. (1992). *Nonlinear Optics*. Academic Press, New York.

Born, M., and Wolf, E. (1999). *Principles of Optics*, 7th ed. Cambridge University Press, Cambridge, UK.

Brink, D. J., and Proch, D. (1982). Efficient tunable ultraviolet source based on stimulated Raman scattering of an excimer-pumped dye laser. *Opt. Lett.* 7, 494–496.

Brosnan, S. J., and Byer, R. L. (1979). Optical parametric oscillator threshold and linewidth studies. *IEEE J. Quantum Electron.* QE-15, 415–431.

Byer, R. L., Oshman, M. K., Young, J. F., and Harris, S. E. (1968). Visible CW parametric oscillator. *Appl. Phys. Lett.* 13, 109–111.

Diddams, S. A., Jones, D. J., Ye, J., Cundiff, S. T., Hall, J. L., Ranka, J. K., Windeler, R. S., Holzwarth, R., Udem, T., and Hänsch, T. W. (2000). Direct link between microwave and optical frequencies with a 300 THz femtosecond laser comb. *Phys. Rev. Lett.* 84, 5102–5105.

Diels, J.-C. (1990). Femtosecond dye lasers. In *Dye Laser Principles* (Duarte, F. J., and Hillman, L. W., eds.). Academic Press, New York, pp. 41–132.

Diels, J.-C., and Rudolph, W. (1996). *Ultrashort Laser Pulse Phenomena*. Academic Press, New York.

Eckstein, J. N., Ferguson, A. I., and Hänsch, T. W. (1978). High-resolution two-photon spectroscopy with picosecond light pulses. *Phys. Rev. Lett.* 40, 847–850.

Fouche, D. G., and Chang, R. K. (1972). Observation of resonance Raman scattering below the dissociation limit in I_2 vapor. *Phys. Rev. Lett.* 29, 536–539.

Giordmaine, J. A., and Miller, R. C. (1965). Tunable coherent parametric oscillation in $LiNbO_3$ at optical frequencies. *Phys. Rev. Lett.* 14, 973–976.

Hanna, D. C., Pacheco, M. T. T., and Wong, K. H. (1985). High efficiency and high brightness Raman conversion of dye laser radiation. *Opt. Commun.* 55, 188–192.

Harris, S. E. (1969). Tunable optical parametric oscillators. *Proc. IEEE* 57, 2096–2113.

Hartig, W., and Schmidt, W. (1979). A broadly tunable IR waveguide Raman laser pumped by a dye laser. *Appl. Phys.* 18, 235–241.

Holzwarth, R., Udem, Th., Hänsch, T. W., Knight, J. C., Wadsworth, W. J., and Russell, P. St. J. (2000). Optical frequency synthesizer for precision spectroscopy. *Phys. Rev. Lett.* 85, 2264–2267.

Holzwarth, R., Zimmermann, M., Udem, T., and Hänsch, T. W. (2001). Optical clockworks and the measurement of laser frequencies with a mode-locked frequency comb. *IEEE J. Quantum Electron.* 37, 1493–1501.

Kumar, P., Shapiro, J. H., and Bondurant, R. S. (1984). Fluctuations in the phase-conjugate signal generated via degenerate four-wave mixing. *Opt. Commun.* 50, 183–188.

Ludewigt, K., Birkmann, K., and Wellegehausen, B. (1984). Anti-Stokes Raman laser investigations on atomic Tl and Sn. *Appl. Phys. B* 33, 133–139.

Manners, J. (1983). XeCl laser-generated infrared SRS in barium vapor. *Opt. Commun.* 46, 366–370.

Marshall, L. H., and Piper, J. A. (1990). Transient stimulated Raman scattering in lead vapor. *IEEE J. Quantum Electron.* 26, 1098–1104.

Mills, D. L. (1991). *Nonlinear Optics.* Springer-Verlag, Berlin.

Milton, T. K., Byer, R. A., Kim, H. L., and Ganiel, J. D. (1990). A tunable, single-mode, LiNbO3 optical parametric oscillator. *Opt. Commun.* 80, 289–293.

Orr, B. J., Johnson, M. J., and Haub, J. G. (1995). Spectroscopic applications of pulsed tunable optical parametric oscillators. In *Tunable Laser Applications* (Duarte, F. J., ed.). Marcel Dekker, New York, pp. 11–82.

Schmidt, W., and Appt, W. (1972). Tunable stimulated Raman emission generated by a dye laser. *Z. Naturforsch.* 27a, 792–793.

Schomburg, H., Döbele, H. F., and Rückle, B. (1983). Generation of tunable narrow-bandwidth VUV radiation by anti-Stokes SRS in H_2. *Appl. Phys. B* 30, 131–134.

Shen, Y. R. (1984). *The Principles of Nonlinear Optics.* Wiley, New York.

Trutna, W. R., and Byer, R. L. (1980). Multiple-pass Raman gain cell. *Appl. Opt.* 19, 301–312.

Trutna, W. R., Park, Y. K., and Byer, R. L. (1979). The dependence of Raman gain on pump laser bandwidth. *IEEE J. Quantum Electron.* QE-15, 648–655.

White, J. C., and Henderson, D. (1983). Tuning and saturation behavior of the anti-Stokes Raman laser. *Opt. Lett.* 8, 15–17.

Wilke, V., and Schmidt, W. (1978). Tunable UV radiation by stimulated Raman scattering. *Appl. Phys.* 16, 151–154.

Wyatt, R., and Cotter, D. (1980). Tunable infrared generation using 6s–5d Raman transition in cesium vapor. *Appl. Phys.* 21, 199–204.

Yariv, A. (1977). Compensation for atmospheric degradation of optical transmission by nonlinear optical mixing. *Opt. Commun.* 21, 49–50.

Yariv, A. (1975). *Quantum Electronics*, 2nd ed. Wiley, New York.

Yariv, A. (1985). *Optical Electronics*, 3rd ed. HRW, New York.